

## Construction of 714 MHz HOM-free accelerating cavities

Shogo Sakanaka,\* Fujio Hinode,† Kiyoshi Kubo and Junji Urakawa

High Energy Accelerator Research Organization (KEK),  
1-1 Oho, Tsukuba-shi, Ibaraki-ken 305, Japan.  
E-mail: sakanaka@mail.kek.jp

(Received 4 August 1997; accepted 3 November 1997)

A new ‘higher-order-mode (HOM)-free’ accelerating cavity has been developed which can provide an accelerating voltage of more than 400 kV per cavity at a frequency of 714 MHz. The harmful HOMs in the cavities, which can induce beam instabilities at high beam currents, were heavily damped by using four special waveguide ports and broadband microwave loads. Two cavities of this design were installed in the 1.54 GeV accelerator test facility (ATF) damping ring at KEK, and successfully stored beams. This cavity will also be very useful for synchrotron light sources. The basic design, characteristics of HOMs and construction of this cavity are reported.

**Keywords:** higher-order modes; coupled-bunch instabilities; HOM-free cavities; damped cavities.

### 1. Introduction

An RF accelerating cavity is one of the essential components for high-energy electron storage rings. The cavities provide the energy lost by synchrotron radiation as well as a longitudinal focusing effect for beams. The accelerating field is usually produced by exciting the lowest resonance mode that corresponds to the TM<sub>010</sub> mode in a cylindrical cavity resonator. The cavities, however, have many other higher-order-mode (HOM) resonances, and some of them are harmful to the beams. For example, TM<sub>0</sub>-like modes have longitudinal electric fields on the beam axis, and they can induce a longitudinal coupled-bunch instability. On the other hand, TM<sub>1</sub>- and TE<sub>1</sub>-like modes have transverse magnetic or electric fields on the beam axis, and they can drive a transverse coupled-bunch instability. In order to attain high beam currents in storage rings, the cure for such instabilities is particularly important. Many techniques to avoid the cavity-induced beam instabilities, such as attaching an HOM damping coupler to the cavity or tuning the HOM frequencies, have been developed for a long time.

A new design concept for the cavity, which is a very promising countermeasure to the cavity-induced instabilities, was proposed by Palmer (1988), Conciauro & Arcioni (1990), and others over the past decade. This type of cavity (called a ‘damped’ or ‘HOM-free’ cavity) is equipped with special ports; this is part of the initial design concept. The HOM power is extracted from the cavity through these ports and then dissipated in microwave absorbers. In this way, the  $Q$  values of harmful HOMs can be reduced by typically three orders of magnitude. As a conse-

quence, both longitudinal and transverse beam-coupling impedances due to the HOMs can be reduced to the same extent. These HOM-free cavities have recently been vigorously developed in many accelerator laboratories for application to high-intensity accelerators, such as linear colliders,  $B$ - or  $\Phi$ -factories and synchrotron light sources.

Based on this design concept, we have developed a 714 MHz HOM-free cavity which was used for the 1.54 GeV electron damping ring of the accelerator test facility (ATF) at KEK. We installed two cavities of this type in the damping ring, and successfully stored beams.

### 2. Basic cavity design

An RF frequency of 714 MHz, just a quarter of the injector-linac RF frequency (2856 MHz), was chosen for the damping ring since this allows us to synchronize the linac and the damping ring RF systems. A single-cell copper cavity, which is equipped with waveguide ports for extracting harmful HOMs, was adopted for the basic design (Sakanaka *et al.*, 1993). We set the cut-off frequency of the waveguide ports to be 1.24 times higher than the accelerating frequency so that the accelerating field is kept in the cavity. Both the cavity inner shape and locations of the waveguide ports were determined so as to damp the HOMs most effectively, while obtaining a reasonably high shunt impedance of the accelerating mode. We first noticed the field distributions of harmful TM<sub>0</sub>, TM<sub>1</sub> and TE<sub>1</sub> modes in a cylindrical pillbox cavity. It can be seen that the circumferential magnetic field components ( $H_\phi$ ) of these modes take maxima at the outermost corners of the cavity. This suggests that if we attach flat (long in the circumferential direction) rectangular waveguides to these corners, the RF fields of such HOMs can be coupled well to the TE<sub>10</sub> propagation mode in the waveguides. Thus, the HOMs can be effectively extracted through the waveguide ports.

The inner shape of an actual cavity, having beam holes, was then designed. The shunt impedance of the accelerating mode was improved by attaching nose cones and rounding outermost corners. During the course of this optimization, we made sure that the field distributions of harmful HOMs were kept similar to those of the pillbox cavity as much as possible. This ensured good coupling of the HOMs to the waveguides. Fig. 1 shows the thus-designed inner shape of the cavity. In order to improve the  $Q$  value of the accelerating mode, the outermost corners were rounded with a modest radius of 30 mm. Although rounding with a larger radius improves the  $Q$  value further, this tends to introduce several HOMs that cannot be damped well. As shown in Fig. 2, principal HOMs in this cavity have a strong magnetic field,  $H_\phi$ , at the location of the waveguide port.

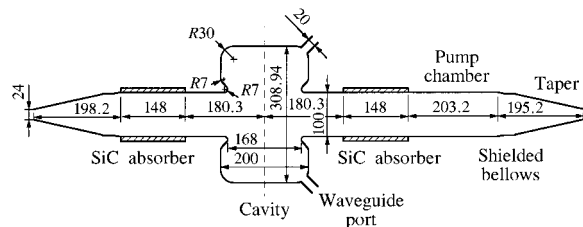


**Figure 1**  
Inner shape of the cavity. Beam-pipe HOM absorbers and taper ducts beside the cavity are also shown. Units: mm.

† Present address: Laboratory for Nuclear Science, Tohoku University, 1-2-1 Mikamine, Taihaku, Sendai, Miyagi 982, Japan.

We attached four waveguide ports to the cavity: two of them are located at the upper and lower positions of one corner, and the other two are located at the left and right positions of the other corner. The cavity is shown schematically in Fig. 3. This configuration allows us to damp both horizontally and vertically polarized dipole modes as well as monopole modes, while keeping a reasonable cavity symmetry ( $180^\circ$  rotational symmetry around the beam axis). Comparing this design with those of PEP-II (Rimmer *et al.*, 1991) and DAΦNE (Bartalucci *et al.*, 1993), which are equipped with three waveguides, there are several advantages: (i) harmful TM<sub>0</sub>-like modes can be damped better; (ii) mechanical design is simpler; (iii) spots of the heat concentration are distributed. In designing the cavity shape, we also ensured that the resonant frequencies of monopole and quadrupole modes are reasonably separated from each other. This is because if the resonant frequencies of these modes are close to each other, these modes are mixed when the waveguide ports are attached, which sometimes results in poor damping of the mixed modes. In addition, we also attached HOM absorbers on a beamline in order to damp the HOMs having very high resonant frequency.

### 3. Investigation of HOM damping

We first investigated the performance of HOM damping by using a three-dimensional electromagnetic simulation code, *MAFIA*. An external  $Q$  value ( $Q_{ex}$ ) of each resonance mode, which measures the coupling to the waveguide ports, was calculated by applying Slater's tuning method together with Kroll–Yu's analysis technique (Kroll & Yu, 1990). The results for the potentially most harmful HOMs (TM<sub>011</sub>-, TM<sub>110</sub>- and TM<sub>111</sub>-like modes) are given in Table 1. It was shown that the external  $Q$  values of these modes were about 7, 24 and 24, respectively, which will be sufficiently small to avoid coupled-bunch instabilities even at the maximum beam current of 600 mA. It was also suggested that the

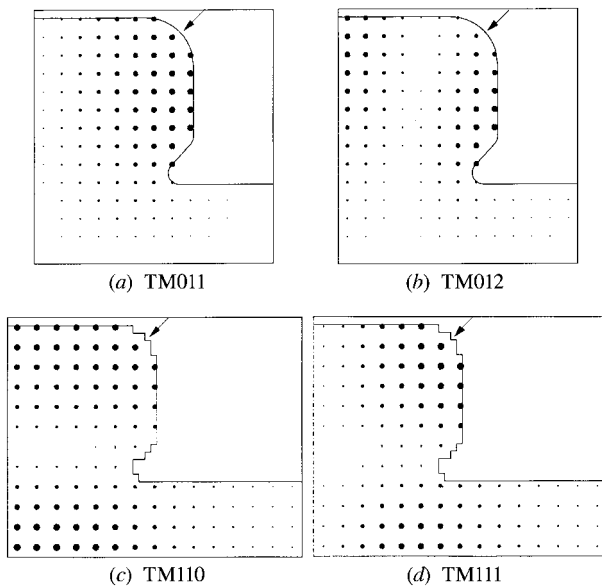


**Figure 2**

Magnetic field distributions for the principal higher-order modes. The location of the waveguide port is shown by arrows. (c) and (d) show one (vertical) polarization of dipole modes; the cross section is cut at a vertical plane ( $x = 0$ ).

**Table 1**

Calculated and measured characteristics of the principal HOMs in the cavity, which was loaded with waveguide ports.

Mode	Calculated $f$ (GHz)	Calculated $Q_{ex}$	Calculated	Measured with
			(without waveguides) $R/Q$ ( $\Omega$ ) or $R_T/Q$ ( $\Omega \text{ m}^{-1}$ )	cold-model $f$ (GHz) $Q_L$
TM <sub>011</sub>	1.075	7.1	$R/Q = 62.5 \Omega$	Not visible
TM <sub>110</sub>	1.160	24	$R_T/Q = 263 \Omega \text{ m}^{-1}$	1.158 24
TM <sub>111</sub>	1.363	24	$R_T/Q = 726 \Omega \text{ m}^{-1}$	1.363 19

other HOMs, up to the beam-hole cut-off frequencies, were damped well.

We further investigated the cavity performance by low-power RF measurements on a cold-model cavity (Sakanaka *et al.*, 1994). The model cavity was equipped with the waveguides, broadband dummy loads and beam-pipe HOM absorbers. We measured the loaded  $Q$  values of the HOMs, and then analysed their field distributions by applying a bead perturbation method. Fig. 4 shows an example of the HOM spectrum measured with a network analyser. We could assign an azimuthal mode index,  $m$ , to each resonance mode, except for a few resonances that almost overlapped each other, in which case applying the perturbation measurement was very difficult. The resultant mode assignment and measured  $Q$  value, together with  $R/Q$  for monopole modes, are given in Fig. 4, where  $R$  is the shunt impedance ( $= V_c^2/P_c$ ,

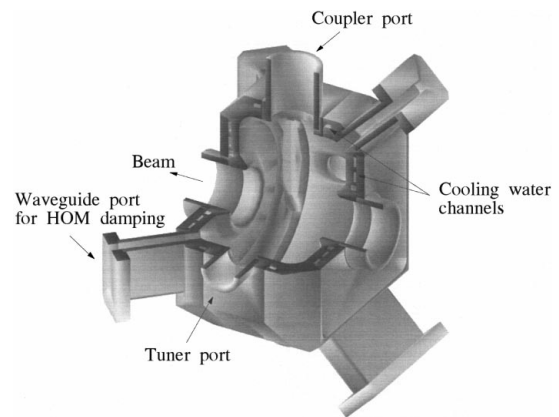


**Figure 3**

Structure of the HOM-free cavity. A quarter of the cavity is cut out to show the inside.

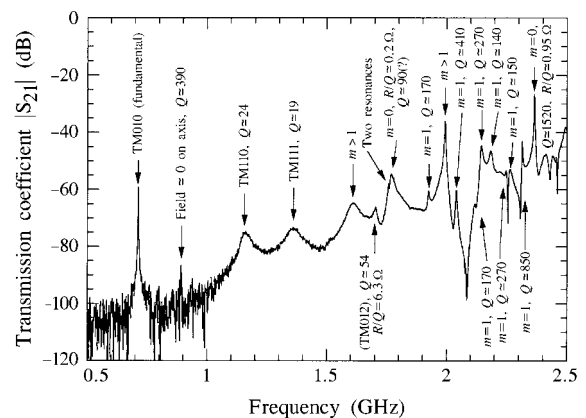


**Figure 4**

Higher-order-mode spectrum of the cold-model cavity. The transmission coefficient between two probes, located at both end plates, was observed.

**Table 2**

Accelerating-mode parameters of the high-power cavity.

Resonant frequency	714 MHz
Unloaded $Q$ (measured)	23000
Shunt impedance, $R (= V_c^2/P_c)$	3.8 M $\Omega$
$R/Q$	166 $\Omega$
Coupling coefficient, $\beta$	2.3
Maximum gap voltage	>400 kV

where  $V_c$  and  $P_c$  are the gap voltage and the wall loss, respectively). The measured loaded  $Q$  values for the principal HOMs agreed fairly well with the calculated external  $Q$  values. The HOM damping performance for other HOMs also seems very good.

#### 4. Construction and operation of the cavities

We then constructed a prototype high-power cavity (Sakanaka *et al.*, 1995). The aim of the design concept was to realize the above cavity scheme using as simple a structure as possible. The basic cavity structure is shown in Fig. 3. Effective cooling was provided by milling water channels directly to the main copper body. We carefully designed the waveguide ports and other ports so that any problems, such as heating up or discharges around the ports, could be avoided. We mainly adopted well established construction techniques, both machining and brazing, to construct the cavity. Other joining techniques, such as electron-beam welding, hot isostatic pressing and TIG welding, were also used auxiliarily. Detailed mechanical design and fabrication were carried out at Keihin Product Operations of Toshiba Corporation. We established fabrication techniques through this construction.

The prototype cavity was then tested under high power (Sakanaka *et al.*, 1996). After conditioning for about 50 h, we successfully fed an input power of 50 kW to the cavity, which was limited by the available klystron power. An estimated accelerating voltage under that condition was about 420 kV per cavity, which was about 1.7 times higher than required for the ATF damping ring. We found no problems during this test.

In parallel with the cavity development, we also developed two types of HOM absorbers, *i.e.* a beam-pipe HOM absorber and a waveguide dummy load (Sakanaka, Hinode *et al.*, 1997). We adopted silicon carbide (SiC) as the microwave absorbing material. The beam-pipe HOM absorber was fabricated by fitting an SiC duct into a copper jacket. The waveguide load was constructed by brazing several SiC tiles into a copper waveguide.

Two additional cavities with the same design as the prototype were manufactured. Table 2 gives the principal parameters of the accelerating mode for these cavities. Each cavity was conditioned on a test bench up to an input power of 44 kW. These cavities were then installed in the damping ring, and conditioned further. The ATF damping ring started commissioning in January 1997,

and the first beam was stored in the ring on 31 January 1997, using these cavities (Sakanaka, Kubo *et al.*, 1997). The ATF damping ring has been operated well from January to July, 1997, and many accelerator studies are underway. The waveguide HOM loads have not been installed at present, but will be installed during the summer shutdown in 1997.

#### 5. Conclusions

714 MHz HOM-free cavities were designed and constructed. Harmful higher-order modes were heavily damped by equipping waveguide ports and dummy loads. The prototype cavity successfully produced an accelerating voltage of about 420 kV per cavity on a test bench. Two additional cavities were installed in the ATF damping ring at KEK, and have been operating well for half a year. This cavity will also be very useful for high-intensity synchrotron light sources.

We would like sincerely to thank Professors K. Takata, Y. Yamazaki and H. Kobayakawa for the promotion of this work and their encouragement. We also thank K. Satoh, T. Miura and Y. Hirata of Toshiba Corporation for manufacturing the cavity, and members of the ATF collaboration team for useful discussions and support.

#### References

- Bartalucci, S., Boni, R., Gallo, A., Palumbo, L., Parodi, R., Serio, M. & Spataro, B. (1993). *Proceedings of the 1993 Particle Accelerator Conference*, pp. 778–780. Piscataway, NJ: IEEE.
- Conciauro, G. & Arcioni, P. (1990). *Proceedings of the Second European Particle Accelerator Conference*, pp. 149–151. Gif-sur-Yvette: Editions Frontières.
- Kroll, N. M. & Yu, D. U. L. (1990). *Part. Accel.* **34**, 231–250.
- Palmer, R. B. (1988). SLAC-PUB-4542. SLAC.
- Rimmer, R., Voelker, F., Lambertson, G., Allen, M., Hodgeson, J., Ko, K., Pendleton, R., Schwarz, H. & Kroll, N. (1991). *Proceedings of the 1991 Particle Accelerator Conference*, pp. 819–821. Piscataway, NJ: IEEE.
- Sakanaka, S., Hinode, F., Akemoto, M., Tokumoto, S., Higo, T., Urakawa, J., Miura, T., Hirata, Y. & Satoh, K. (1995). *Proceedings of the 1995 Particle Accelerator Conference*, pp. 1788–1790. Piscataway, NJ: IEEE.
- Sakanaka, S., Hinode, F., Kubo, K., Akemoto, M. & Urakawa, J. (1996). *Proceedings of the Fifth European Particle Accelerator Conference*, pp. 2017–2019. Bristol: Institute of Physics.
- Sakanaka, S., Hinode, F., Kubo, K., Higo, T., Urakawa, J. & Rizawa, T. (1994). *Proceedings of the 1994 International Linac Conference*, pp. 281–283. Tsukuba, Ibaraki: KEK.
- Sakanaka, S., Hinode, F., Kubo, K., Tokumoto, S., Satoh, K., Miura, T. & Naba, T. (1997). KEK Preprint 97–25. KEK, Tsukuba, Ibaraki 305, Japan.
- Sakanaka, S., Kubo, K. & Higo, T. (1993). *Proceedings of the 1993 Particle Accelerator Conference*, pp. 1027–1029. Piscataway, NJ: IEEE.
- Sakanaka, S., Kubo, K., Hinode, F., Hayano, H., Urakawa, J. & Minty, M. G. (1997). KEK Preprint 97–26. KEK, Tsukuba, Ibaraki 305, Japan.